DTIC FILE COPY

UNCLASSIFIED

1

AD-A201 363

REPORT DOCUMENTATION PAGE

1b. RESTRICTIVE MARKINGS	
2b. DECLASSIFICATION/DOWNGRADING SCHEDULE	3. DISTRIBUTION/AVAILABILITY OF REPORT
4. PERFORMING ORGANIZATION REPORT NUMBER(S) FJSRL-JR-88-0012	5. MONITORING ORGANIZATION REPORT NUMBER(S)
6a. NAME OF PERFORMING ORGANIZATION Frank J. Seiler Research Lab; 6b. OFFICE SYMBOL (If applicable) FJSRL/NH	7a. NAME OF MONITORING ORGANIZATION
6c. ADDRESS (City, State and ZIP Code) USAF Academy Colorado Springs, CO 80840-6528	7b. ADDRESS (City, State and ZIP Code)
8a. NAME OF FUNDING/SPONSORING ORGANIZATION; 8b. OFFICE SYMBOL (If applicable)	9. PROCUREMENT INSTRUMENT IDENTIFICATION NUMBER
8c. ADDRESS (City, State and ZIP Code)	10. SOURCE OF FUNDING NOS. PROGRAM ELEMENT NO. / PROJECT NO. / TASK NO. / WORK UNIT NO.

DTIC ELECTE OCT 1 9 1988 S E D

11. TITLE (Include Security Classification) Integral Solution for Diffraction Problems Involving Conducting Surfaces with Complex Geometries. III. Application to Paraboloidal Mirrors (U)

12. PERSONAL AUTHOR(S) Mohamed F. El-Hewie

13a. TYPE OF REPORT	13b. TIME COVERED	14. DATE OF REPORT (Yr., Mo., Day)	15. PAGE COUNT
Journal Publication	FROM ____ TO ____	September 1988	6

16. SUPPLEMENTARY NOTATION

17. COSATI CODES			18. SUBJECT TERMS (Continue on reverse if necessary and identify by block number)
FIELD	GROUP	SUB. GR.	paraboloidal mirrors, diffraction, ray tracing

19. ABSTRACT (Continue on reverse if necessary and identify by block number)

The complex ray-tracing theory developed earlier (J. Opt. Soc. Am. A 5, 200 (1988)) is applied to a study of the structure of the electromagnetic focal field spectrum of paraboloidal ~~mirrors. This problem~~ was treated recently by Barakat (Appl. Opt. 26, 3790 (1987)), who used the Gaussian vectorial diffraction method. In this paper a more general solution to the problem is presented that uses the Stratton-Chu-Silver integral. The reflecting kernel then explicitly incorporates the surface function, the surface physical parameters and their dependence on the state of polarization of the incident radiation, and an unrestricted aberration function. Numerical results are presented for mirrors made of four different metals, and their use in optimizing the mirror is demonstrated.

20. DISTRIBUTION/AVAILABILITY OF ABSTRACT	21. ABSTRACT SECURITY CLASSIFICATION
UNCLASSIFIED/UNLIMITED ☒ SAME AS RPT. ☒ DTIC USERS ☐	UNCLASSIFIED

22a. NAME OF RESPONSIBLE INDIVIDUAL	22b. TELEPHONE NUMBER (Include Area Code)	22c. OFFICE SYMBOL
Mohamed F. El-Hewie	719-472-3122	FJSRL/NH

DD FORM 1473, 83 APR EDITION OF 1 JAN 73 IS OBSOLETE. UNCLASSIFIED

SECURITY CLASSIFICATION OF THIS PAGE

FJSRL-JR-88-0012

Reprinted from Journal of the Optical Society of America A, Vol. 5, page 1444, September 1988

Integral solution for diffraction problems involving conducting surfaces with complex geometries. III. Application to paraboloidal mirrors

Mohamed F. El-Hewie

Frank J. Seiler Research Laboratory, U.S. Air Force Academy, Colorado Springs, Colorado 80840-6528

Received October 26, 1987; accepted May 6, 1988

The complex ray-tracing theory developed earlier [J. Opt. Soc. Am. A 5, 200 (1988)] is applied to a study of the structure of the electromagnetic focal field spectrum of paraboloidal mirrors. This problem was treated recently by Barakat [Appl. Opt. 26, 3790 (1987)], who used the Gaussian vectorial diffraction method. In this paper a more general solution to the problem is presented that uses the Stratton–Chu–Silver integral. The reflecting kernel then explicitly incorporates the surface function, the surface physical parameters and their dependence on the state of polarization of the incident radiation, and an unrestricted aberration function. Numerical results are presented for mirrors made of four different metals, and their use in optimizing the mirror design is demonstrated.

INTRODUCTION

In part I of this series a complex ray-tracing theory was developed for the solution of diffraction problems of complex conducting surfaces.[1] In part II the theory was applied to the ellipsoidal scatterers.[2] Recently Barakat[3] studied the structure of the focal spectrum of a paraboloidal mirror, assuming that the mirror is absolutely reflecting, the incident rays are symmetrical and meridional, and the system is aberration free. In what follows it is shown that these assumptions can easily be eliminated without adding much complexity to the method of solution.

First, if the mirror is metallic, the real refractive index varies with the angle of incidence. For example, at radiation wavelengths $\lambda = 0.1$ μm and $\lambda = 1.315$ μm the real refractive index of aluminum is, respectively, 14.64 and 1.00 at normal incidence and 14.66 and 1.06 at grazing incidence.[2] Thus the reflectivity and absorptivity vary with the angle of ray incidence upon a metallic surface, and both vary with the state of wave polarization for both metallic and dielectric surfaces.[2,4] Therefore the conservation of energy in a ray tube [Ref. 5, Eq. (2.11)] and that carried out by Barakat [Ref. 3, Eq. (14)] should yield the polarization and angular dependence of the surface reflectivity in the aperture function, $q(\theta)$. Second, asymmetrical reflective focusing is of more interest in practice. Inertial confinement fusion devices, in which the laser beams strike the focusing mirrors obliquely, and astrophysical observatories, for which unobstructed images are desired, are just two practical examples. Because in Barakat's approach the Kirchhoff integral is evaluated on a Gaussian sphere centered at the Gaussian focus, asymmetrical focusing can hardly be analyzed by his approach. Third, the intended inclusion of some aberration orders, third-order spherical and third-order coma, can easily be replaced by the whole aberration function by using the Stratton–Chu–Silver integral in place of the Kirchhoff integral.

In this paper a general treatment is presented for the focusing of a plane wave and a Gaussian laser beam by an aluminum-coated paraboloidal mirror. Three other metal coatings are studied for comparison with aluminum. The surface geometrical and physical parameters, the state of radiation polarization, and the whole wave-front-aberration function are explicitly incorporated into the reflecting kernel.

MATHEMATICAL FORMULATION

The equations of parts I and II, respectively, cited here will be preceded by the numerals I and II. Given a plane wave with a propagation constant $k = 2\pi/\lambda$ and a propagation unit vector $\hat{n}_i$, Eq. (I.10a) gives

$$q(Z, \sigma, \omega) = -(\xi\Psi - \zeta\Lambda)/k + [\sin\theta_i(Z_x \cos\varphi_i + Z_y \sin\varphi_i) - \cos\theta_i]/(1 + Z_x{}^2 + Z_y{}^2)^{1/2}. \quad (1)$$

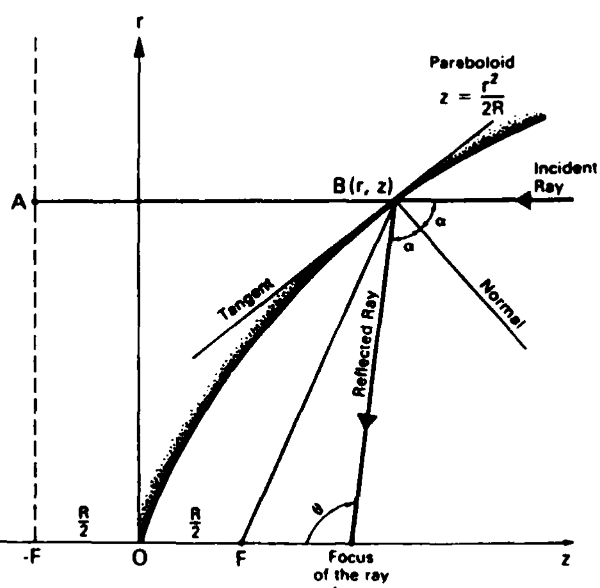

Fig. 1. Geometry of the problem.

88 10 18 151

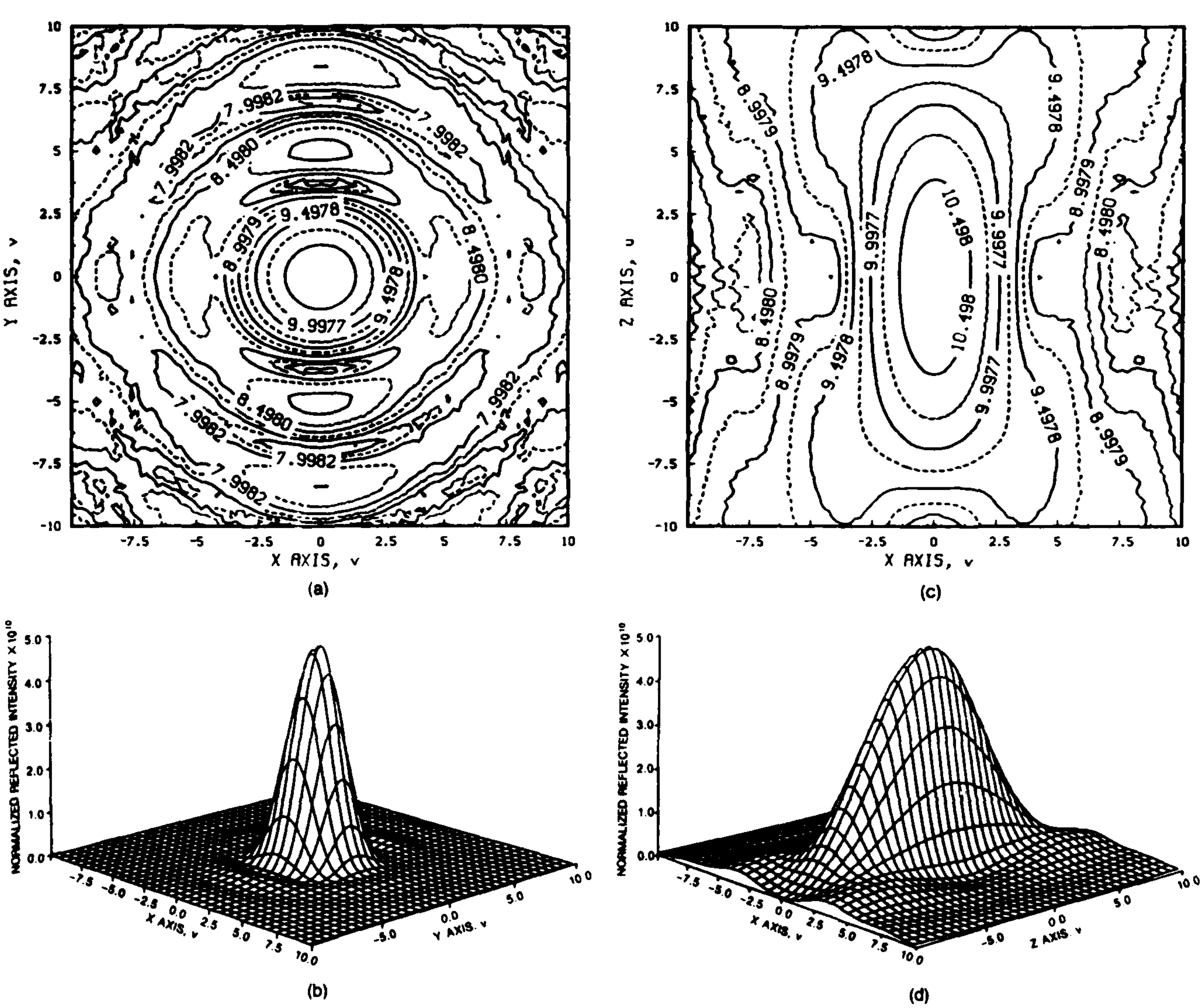

Fig. 2. Results of Ref. 3, Figs. 10–12, reproduced, using our computational code, with a perfectly reflecting paraboloidal mirror with a focal length of $R/2 = 50$ cm and a height of $d = 10$ cm. The following notation is used: $v = kx \sin\alpha$ on the x axis and $v = ky \sin\alpha$ on the y axis, $\sin\alpha = (2Rd)^{1/2}/(R/2)$, and $u = kz \sin^2\alpha$. (a) Contours of the reflected energy in the xy plane at the focus, $z = -R/2$ (the contour labels are $\log_{10}$ of the reflected energy normalized to the maximum incident energy). (b) Surface plot of the energy in the xy focal plane. (c), (d) Correspond to (a) and (b), respectively, but in the xz plane with $z = 0$ in these figures corresponding to the focal point in Fig. 1.

Equations (I.8) then give $\Psi(Z, \sigma, \omega)$ and $\Lambda(Z, \sigma, \omega)$ in terms of the local angle of incidence θ_{in}, defined below by Eq. (6).

The incident electromagnetic fields have field strength distribution $E_i(Z)$ and aberration function $\mathbf{u}(Z)$ given as follows.

For a plane wave,

$$E_i(Z) = E_0 \exp(-ikw) \tag{2a}$$

and

$$\mathbf{u} = 0. \tag{2b}$$

For a Gaussian beam,[6]

$$E_i(Z) = E_0(w_0/w_i)\exp[-(r/w_i)^2 - ik(w - |\mathbf{u}|)] \tag{2c}$$

and

$$\mathbf{u} = [(1/k)\tan^{-1}(2w/kw_0^2) - r^2/2\rho]\hat{n}_i. \tag{2d}$$

Here, w is the axial distance along the laser beam, measured from the beam waist; w_0 is the beam-waist parameter; w_i is a beam parameter defined by $w_i^2 = w_0^2[1 + (2w/kw_0^2)^2]$; r is the radial distance in the beam frame of coordinates; and ρ is the wave-front curvature at the distance w and is given by $\rho = w + (kw_0^2/2)^2/w$. Thus the F's in Eqs. (I.14) are determined as follows:

For a plane wave,

$$F_1 = \sin\theta_i \cos\varphi_i, \tag{3a}$$

$$F_2 = \sin\theta_i \sin\varphi_i, \tag{3b}$$

and

$$F_3 = \cos\theta_i; \tag{3c}$$

For a Gaussian laser beam,

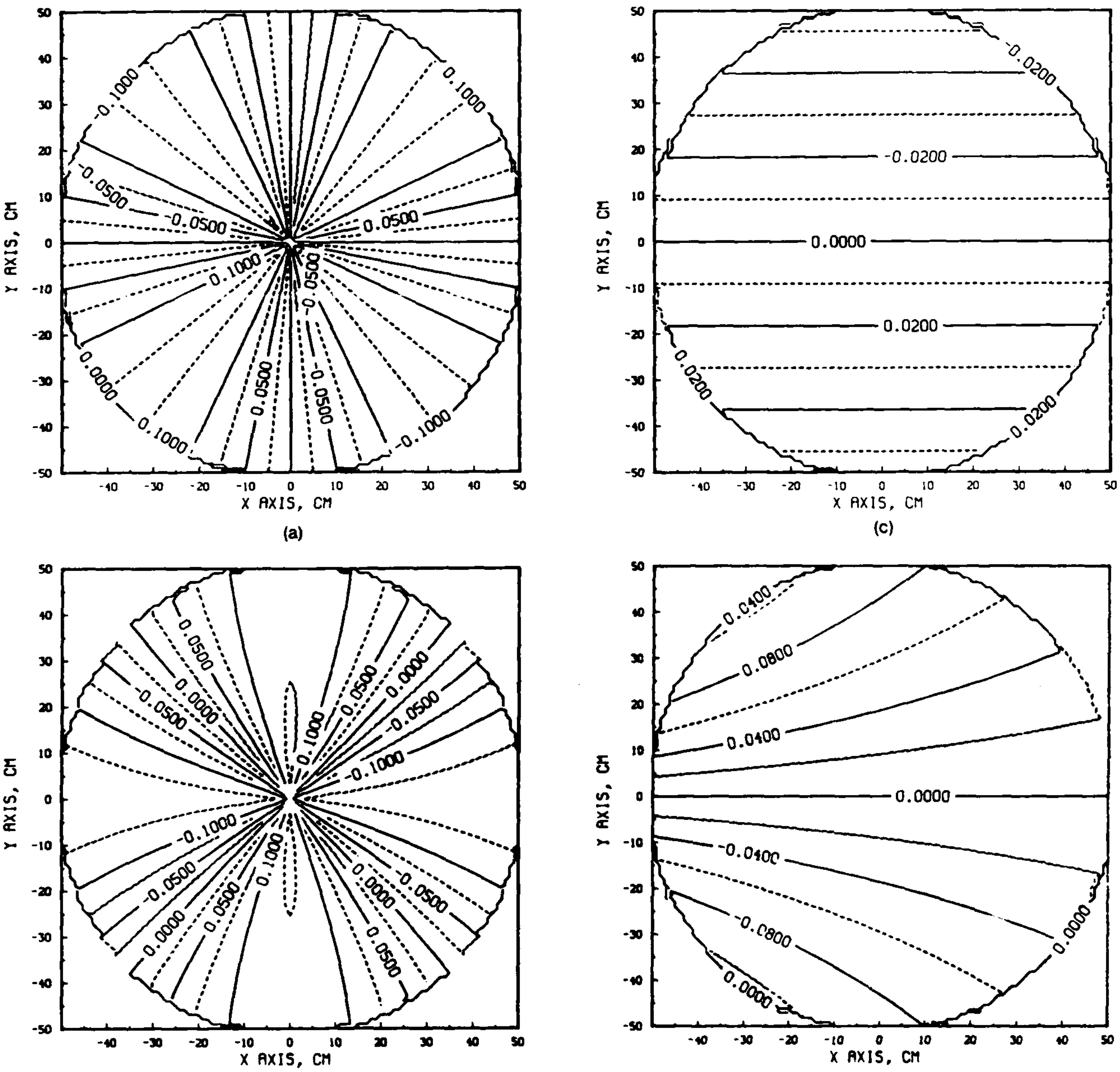

(a) (b) (c) (d)

$$F_1 = \sin\theta_i \cos\varphi_i[1 + (1/k)\tan^{-1}(2w/kw_0^2) - r^2/2(w-\rho)], \tag{3d}$$

$$F_2 = \sin\theta_i \sin\varphi_i[1 + (1/k)\tan^{-1}(2w/kw_0^2) - r^2/2(w-\rho)], \tag{3e}$$

and

$$F_3 = \cos\theta_i[1 + (1/k)\tan^{-1}(2w/kw_0^2) - r^2/2(w-\rho)]. \tag{3f}$$

Now, the coordinate function of a paraboloidal mirror (Fig. 1) can be written in the beam frame ($Z = -z$) as

$$Z = -(x^2 + y^2)/2R \qquad \text{for } -d \leq Z \leq 0, \tag{4}$$

where $R/2$ is the focal length of the paraboloidal mirror. The origin of the frame of coordinates is taken at the vertex of the paraboloid, and the z axis is its axis of revolution. The spatial derivatives of Z are

$$Z_x = -x/R \tag{5a}$$

and

$$Z_y = -y/R. \tag{5b}$$

The local angle of incidence is defined by

$$\cos\theta_{\text{in}} = [-\sin\theta_i(Z_x \cos\varphi_i + Z_y \sin\varphi_i) + \cos\theta_i]/(1 + Z_x^2 + Z_y^2)^{1/2}. \tag{6}$$

Substituting the F's, Z_x, and Z_y from Eqs. (3) and (5) into Eqs. (1) and (I.15) gives the real part of the complex refractive index, ν, for the surface $Z(x, y)$ as a function in Z, Z_x, Z_y, σ, and $\mathbf{u}$.

The Fresnel coefficients of reflection and transmission, written in terms of ν, are then determined in a form similar to Eqs. (II.9). Then Eqs. (I.19) give the various field vectors $\mathbf{e}_s^i$, $\mathbf{h}_s^i$, $\mathbf{e}_p^i$, and $\mathbf{h}_p^i$, and Eqs. (I.21) and (I.22) give the local

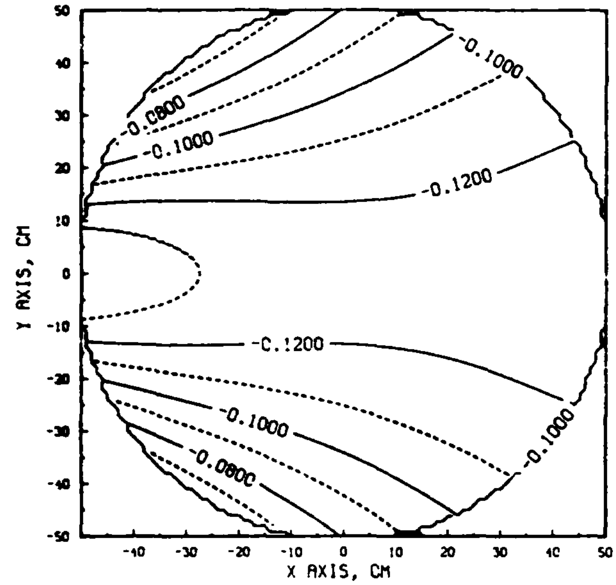

(e)

Fig. 3. The S's [surface currents at an aluminum paraboloidal mirror surface, Eqs. (10)]. (a)–(c) Are for $\theta_i = 0$ incidence, and (d), (e) are for 45° incidence in the $\varphi_i = 0$ plane. (a), (d), S_1. (b), (e) S_2. (c) S_3.

currents on the surface Z, $J_s{}^i$ and $J_p{}^i$. Thus both absorption and reflecting parameters at the surface are fully determined.

To simplify numerical calculations, only the case of a plane wave incident at $\theta_i = 0$, $\varphi_i = 0$, and $\alpha = 0$ will be considered. For this case, Eqs. (I.18) give

$$\hat{t} = [\hat{i}Z_y \cos\theta_i - \hat{j}(\sin\theta_i + Z_x \cos\theta_i) - \hat{k}Z_y \sin\theta_i]/C \sin\theta_{in}, \tag{7a}$$

$$\hat{p} = \{\hat{i}[\sin\theta_i(Z_y{}^2 + 1) + Z_x \cos\theta_i] + \hat{j}[-Z_x Z_y \sin\theta_i + Z_y \cos\theta_i] + \hat{k}[\cos\theta_i(Z_x{}^2 + Z_y{}^2) + Z_x \sin\theta_i]\}/C^2 \sin\theta_{in}, \tag{7b}$$

$$\cos\theta_{in} = (\cos\theta_i - Z_x \sin\theta_i)/(1 + Z_x{}^2 + Z_y{}^2)^{1/2}, \tag{7c}$$

$$\hat{a}\cdot\hat{t} = -Z_y/C \sin\theta_{in}, \tag{7d}$$

$$\hat{a}\cdot\hat{n} = (Z_x \cos\theta_i + \sin\theta_i)/C, \tag{7e}$$

and

$$\hat{a}\cdot\hat{p} = [Z_x(2\sin^2\theta_i + Z_x \sin\theta_i \cos\theta_i - 1) - \sin\theta_i \cos\theta_i]/C^2 \sin\theta_{in}. \tag{7f}$$

Thus all the field components in the incident partial electromagnetic waves at the surface $Z(x, y)$ are also fully determined.

At a point $P(x_p, y_p, z_p)$ external to the surface $Z(x, y)$, the reflected field is given by Eq. (I.30). The unit vectors $\hat{n}$ and $\hat{n}_p$ are given by

$$\hat{n} = (-Z_x\hat{i} - Z_y\hat{j} + \hat{k})/(1 + Z_x{}^2 + Z_y{}^2)^{1/2} \tag{8a}$$

and

$$\hat{n}_p = [(x - x_p)\hat{i} + (y - y_p)\hat{j} + (Z - z_p)\hat{k}]/D, \tag{8b}$$

where $D = [(x - x_p)^2 + (y - y_p)^2 + (Z - z_p)^2]^{1/2}$.

Substituting the $\mathbf{e}^i$'s and $\mathbf{h}^i$'s from Eqs. (I.19) into Eqs. (I.31) and (I.32), we get expressions similar to Eqs. (II.17) for the surface currents as

$$\hat{n} \times \mathbf{e}_s = (E_i/C)(S_1\hat{i} + S_2\hat{j} + S_3\hat{k}) \tag{9a}$$

and

$$\hat{n} \times \mathbf{h}_s = (E_i/\eta C)(T_1\hat{i} + T_2\hat{j} + T_3\hat{k}). \tag{9b}$$

The S's and the T's (the dimensionless parameters that account for the physical and geometrical properties of the surface, the degree of polarization, and the radiation wavelength) are now defined as

$$S_1 = W(-Z_y L_3 - L_2) + \cos\theta_{in}(1 - R_p)M_1, \tag{10a}$$

$$S_2 = W(Z_x L_3 + L_1) + \cos\theta_{in}(1 - R_p)M_2, \tag{10b}$$

$$S_3 = W(-Z_x L_2 + Z_y L_1) + \cos\theta_{in}(1 - R_p)M_3, \tag{10c}$$

$$T_1 = [(1 + R_p)/C](-Z_y M_3 - M_2) - UL_1, \tag{10d}$$

$$T_2 = [(1 + R_p)/C](Z_x M_3 + M_1) - UL_2, \tag{10e}$$

and

$$T_3 = [(1 + R_p)/C](-Z_x M_2 + Z_y M_1) - UL_3. \tag{10f}$$

By executing the vectorial multiplication in Eqs. (I.31) and (I.32), we get

$$W = \hat{a}\cdot\hat{t}(1 + R_s)/C \sin\theta_{in}, \tag{11a}$$

$$U = \hat{a}\cdot\hat{t}(1 - R_s)\cos\theta_{in}/\sin\theta_{in}. \tag{11b}$$

From the expression of $\mathbf{e}_s{}^i$, Eq. (I.19a), we get

$$L_1 = Z_y \cos\theta_i, \tag{11c}$$

$$L_2 = -(\sin\theta_i + Z_x \cos\theta_i), \tag{11d}$$

and

$$L_3 = -Z_y \sin\theta_i. \tag{11e}$$

From the expression of $\mathbf{h}_p{}^i$, Eq. (I.19d), we get

$$M_1 = -K_2 \cos\theta_i, \tag{11f}$$

$$M_2 = K_1 \cos\theta_i - K_3 \sin\theta_i, \tag{11g}$$

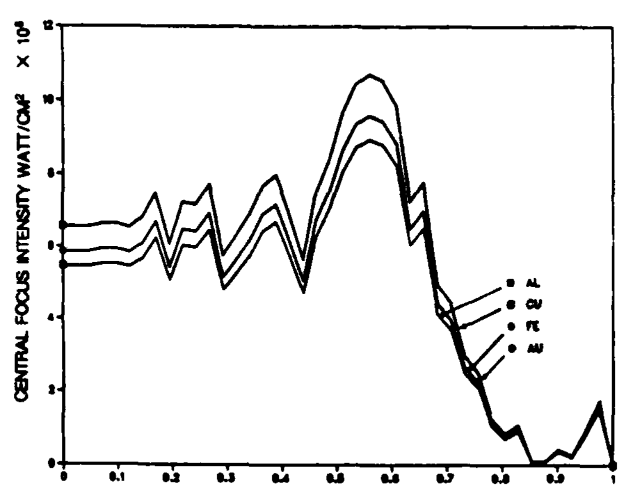

Fig. 4. Effect of the relative central obstruction of the paraboloidal mirror on the focal intensity ($x_p = 0$, $y_p = 0$, $z_p = R$) for four metals.

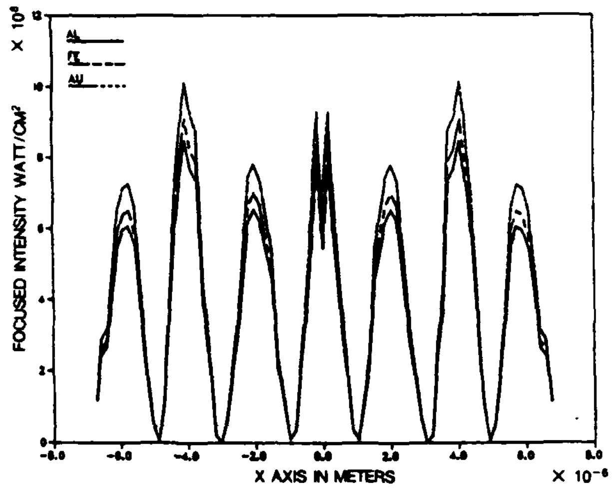

Fig. 5. Intensity distribution along the x axis in the focal plane for the four metals.

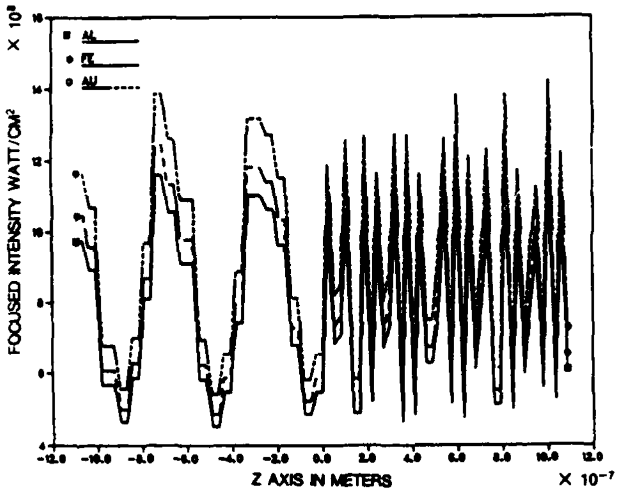

Fig. 6. Intensity distribution along the z axis in the focal volume for the four metals. $z = 0$ in this figure corresponds to the focal point in Fig. 1.

and

$$M_3 = K_2 \sin \theta_i. \tag{11h}$$

From the expression of $\mathbf{e}_p{}^i$, Eq. (I.19c), we get

$$K_1 = -\hat{a} \cdot \hat{n} Z_x + \hat{a} \cdot \hat{p}[\sin \theta_i (Z_y{}^2 + 1) + Z_x \cos \theta_i]/C \sin \theta_{\text{in}}, \tag{11i}$$

$$K_2 = -\hat{a} \cdot \hat{n} Z_y + \hat{a} \cdot \hat{p}(-Z_x Z_y \sin \theta_i + Z_y \cos \theta_i)/C \sin \theta_{\text{in}}, \tag{11j}$$

and

$$K_3 = \hat{a} \cdot \hat{n} + \hat{a} \cdot \hat{p}[(Z_x{}^2 + Z_y{}^2)\cos \theta_i + Z_x \sin \theta_i]/C \sin \theta_{\text{in}}. \tag{11k}$$

Substituting the surface derivatives from Eqs. (5) and the vectorial products from Eqs. (7) into Eqs. (10) and (11), we get expressions for the S's and the T's in terms of the surface coordinates. Then the surface currents that contribute to the reflected fields at P are given by Eqs. (II.20). The three components of the reflected electric field at $P(x_p, y_p, z_p)$ are obtained by substituting the surface currents into Eq. (I.30). The results are

$$\begin{aligned} E_{sx}(P) = &-[ik \exp(-ikD_0)/4\pi D_0] \iint_{\Omega_r} [E_i(Z)/D^2]\cos^2 \theta_{\text{in}} \\ &\times \{[(y - y_p)S_3 - (Z - z_p)S_2]D - [(x - x_p) \\ &\times (Z - z_p)T_3 - [(y - y_p)^2 + (Z - z_p)^2]T_1 \\ &+ (x - x_p)(y - y_p)T_2]\}\exp(ik\Phi)\mathrm{d}x\mathrm{d}y, \end{aligned} \tag{12a}$$

$$\begin{aligned} E_{sy}(P) = &-[ik \exp(-ikD_0)/4\pi D_0] \iint_{\Omega_r} [E_i(Z)/D^2]\cos^2 \theta_{\text{in}} \\ &\times \{[(Z - z_p)S_1 - (x - x_p)S_3]D - [(x - x_p) \\ &\times (y - y_p)T_1 - [(x - x_p)^2 + (Z - z_p)^2]T_2 \\ &+ (y - y_p)(Z - z_p)T_3]\}\exp(ik\Phi), \end{aligned} \tag{12b}$$

and

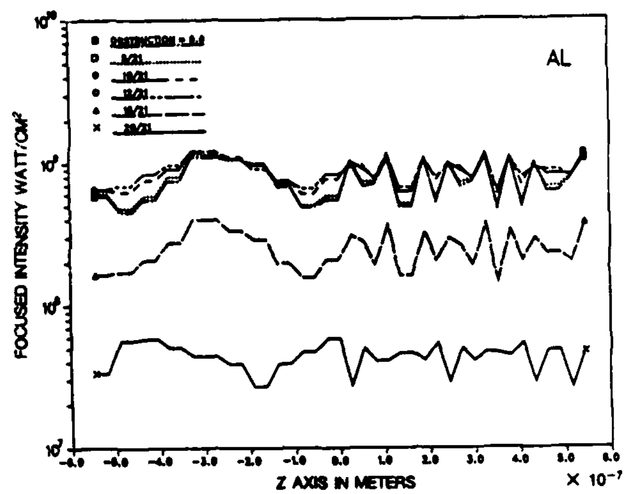

Fig. 7. Effect of the relative obstruction on the z-axial intensity distribution for an aluminum mirror. $z = 0$ in this figure corresponds to the focal point in Fig. 1.

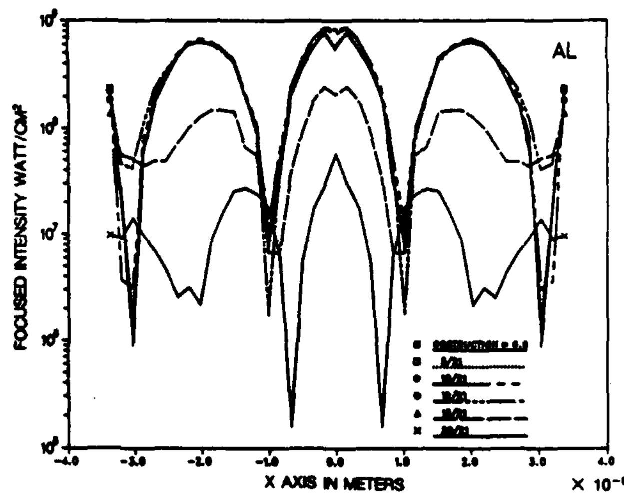

Fig. 8. Effect of the relative obstruction on the x-axial intensity distributions for an aluminum mirror.

$$
\begin{aligned}
E_{sz}(P) = -[ik \exp(-ikD_0)/4\pi D_0] \iint_{\Omega_s} [E_i(Z)/D^2]\cos^2\theta_{\text{in}} \\
\times \{[(x-x_p)S_2 - (y-y_p)S_1]D - [(y-y_p) \\
\times (Z-z_p)T_2 - [(x-x_p)^2 + (y-y_p)^2]T_3 \\
+ (x-x_p)(Z-z_p)T_1]\}\exp(ik\Phi),
\end{aligned}
\tag{12c}
$$

where D_0 is the distance from the origin to the observation point and Φ is given by

$$\Phi = \mathbf{r}\cdot\hat{n}_p = [x(x-x_p) + y(y-y_p) + Z(Z-z_p)]/D. \tag{12d}$$

The solid angle Ω_s is defined in Ref. 2.

The integrals in Eqs. (12) are the Stratton–Chu–Silver intergrals. They offer the following advantages over the Kirchhoff integrals: (a) the physical properties of the reflector are explicitly included in the reflecting kernel, while that used by Barakat, $q(\theta) = 2/(1 + \cos\theta)$, ignores any surface effect; (b) the geometrical surface function is also explicitly included in the reflecting kernel, which permits the treatment of any reflecting geometry; (c) the incident rays need not be parallel, meridional, or symmetrical; (d) integration is carried out on the surface function, not on a Gaussian sphere, permitting the treatment of asymmetrical focusing; and (e) the effect of the thickness of the metallic layer can easily be investigated in a parametric study for the engineering design of paraboloidal mirrors. The last-named issue was treated in Ref. 7 by using the Debye potential solution of the scalar wave equation. The Debye potential approach can be partly applied to our problem if the thickness of the metallic coating is to be optimized. In the region of the metallic coating of few tens of angstroms, ray-tracing geometric optics is of no use.

NUMERICAL RESULTS

First, the results obtained by Barakat (Ref. 3, Figs. 10–12) are reproduced, using the Kirchhoff diffraction method with a perfectly reflecting paraboloidal mirror with a focal length of $R/2 = 50$ cm and a height of $d = 10$ cm along the mirror axis of revolution.[a] The Kirchhoff integrals were evaluated by a numerical double-integration algorithm, using eight-point Newton–Cotes quadratures. We evaluated the integrals without using the Bessel function formulas used in Refs. 3 and 5. Our results are in a good agreement with those obtained in Ref. 3 and are displayed in Fig. 2.

In Fig. 3 the surface currents, the S's, are shown for both symmetrical and oblique incidence. The figures are intended to demonstrate the response of the physical parameters of a metallic mirror to the two angles of incidence. In Fig. 3 and the figures that follow, $\lambda = 1.315\ \mu$m.

Figure 4 shows the effect of the relative central obstruction of the paraboloidal mirror on the focal intensity ($x_p = 0$, $y_p = 0$, $z_p = R$) for four metals. At 0.55, central obstruction the focal intensity is maximum. Copper and silver, as expected, show the highest focal intensity, while aluminum shows the lowest focal intensity. The peaking of the focal intensity that is produced by using a specific ring aperture was proved by others, both experimentally and theoretically, and was used in Ref. 8 to produce a diffraction-free beam.

Figure 5 shows the symmetry of the intensity distribution along the x and z axes in the focal volume for the four metals. Figure 6 shows the asymmetry along the z-axis intensity distribution for the four metals.

Figures 7 and 8 show the effect of the relative obstruction on the axial and perpendicular intensity distributions for an aluminum mirror.

CONCLUSION

In an application of the theory developed in part I, an analysis of the structure of the electromagnetic field spectrum at the focal volume of an aluminum-coated paraboloidal mirror is presented. This is done by replacing the Kirchhoff diffraction integral by the Stratton–Chu–Silver integral. The latter is more appropriate for the study of the diffraction problems by reflectors of complex shapes and physical parameters. This permits the inclusion of the surface physical and geometrical parameters and the full aberration function in the reflecting kernel. The numerical results obtained are in good agreement with Barakat's results in the special case of a perfectly reflecting mirror. We have demonstrated the effects of the central obstruction on the focal intensity distribution for four practical metallic mirrors. The numerical results demonstrate the use of the analytical expressions obtained in Eqs. (12) in the material selection and design of real telescopic mirrors with metallic coating.

REFERENCES

1. M. F. El-Hewie and R. J. Cook, "Integral solution for diffraction problems involving conducting surfaces with complex geometries. I. Theory," J. Opt. Soc. Am. A 5, 200–205 (1988).
2. M. F. El-Hewie and D. Fredal, "Integral solution for diffraction problems involving conducting surfaces with complex geometries. II. Application to ellipsoidal surfaces," J. Opt. Soc. Am. A 5, 1105–1117 (1988).
3. R. Barakat, "Diffracted electromagnetic fields in the neighborhood of a paraboloidal mirror having a central obscuration," Appl. Opt. 26, 3790–3795 (1987).
4. M. Born and E. Wolf, *Principles of Optics*, 6th ed. (Pergamon, New York, 1980).
5. B. Richard and W. Wolf, "Electromagnetic diffraction in optical systems. II. Structure of the image field in an aplanatic system," Proc. R. Soc. London Ser. A 253, 258–281 (1959).
6. H. Kogelnik and T. Li, "Laser beams and resonators," Appl. Opt. 5, 1550–1567 (1966).
7. A. B. Pluchino, "Surface waves and the radiative properties of micron-sized particles," Appl. Opt. 20, 2986–2992 (1981).
8. J. Durnin, J. J. Miceli, Jr., and J. H. Eberly, "Diffraction-free beams," Phys. Rev. Lett. 58, 1499–1501 (1987).